Stability, dynamics, and tolerance to undersaturation of surface nanobubbles

Tan, Beng Hau; An, Hongjie; Ohl, Claus-Dieter

2019

Tan, B. H., An, H., & Ohl, C.-D. (2019). Stability, dynamics, and tolerance to undersaturation of surface nanobubbles. Physical Review Letters, 122(13), 134502-. doi:10.1103/PhysRevLett.122.134502

https://hdl.handle.net/10356/105417

https://doi.org/10.1103/PhysRevLett.122.134502

Stability, Dynamics, and Tolerance to Undersaturation of Surface Nanobubbles

Beng Hau Tan,[1] Hongjie An,[2,3,*] and Claus-Dieter Ohl[4,†]

[1]Low Energy Electronic Systems, Singapore-MIT Alliance for Research and Technology, 1 Create Way, 138602 Singapore
[2]Queensland Micro and Nanotechnology Centre, Griffith University, 170 Kessels Road, Nathan, Queensland 4111, Australia
[3]Division of Physics and Applied Physics, School of Physical and Mathematical Sciences, Nanyang Technological University, 21 Nanyang Link, 637371 Singapore
[4]Otto von Guericke University Magdeburg, Institute of Experimental Physics, Universitätsplatz 2, 39016 Magdeburg, Germany

(Received 28 January 2019; revised manuscript received 4 March 2019; published 5 April 2019)

The theoretical understanding of surface nanobubbles—nanoscale gaseous domains on immersed substrates—revolves around two contrasting perspectives. One perspective, which considers gas transport in the nanobubbles' vicinity, explains numerous stability-related properties but systematically underestimates the dynamical response timescale by orders of magnitude. The other perspective, which considers gas transport as the bulk liquid equilibrates with the external environment, recovers the experimentally observed dynamical timescale but incorrectly predicts that nanobubbles progressively shrink until dissolution. We propose a model that couples both perspectives, which is capable of explaining the stability, dynamics, and unexpected tolerance of surface nanobubbles to undersaturated environments.

DOI: 10.1103/PhysRevLett.122.134502

Surface nanobubbles are long-lived, gaseous domains found on immersed hydrophobic substrates [1–5]. Their discovery two decades ago was greeted with scepticism, as nanobubbles were claimed to have lifetimes many orders longer than predicted by the well-established theory of Epstein and Plesset [6]. While the existence of the nanobubbles is now undoubted, no single theory explains all of their unusual properties.

In the past decade, the theoretical understanding of surface nanobubbles has coalesced around two contrasting perspectives. The first perspective focuses on gas transport throughout the bulk liquid. Weijs and Lohse [7] treat a newly nucleated nanobubble as a source of gas oversaturation, which dissipates by diffusion as the liquid equilibrates to saturation. As gas transport occurs within a liquid pool with characteristic length ℓ, the *global diffusion timescale* is $\tau_G \sim \ell^2/D$ (D is the diffusion constant). As the authors note, $\tau_G \sim 10$ hr, if $\ell \sim 1$ cm. However, surface nanobubbles are predicted to shrink progressively until they dissolve at τ_G, which is at odds [8] with the experimental finding that they exhibit little change in morphology over many days [3,9].

Alternatively, Lohse and Zhang [10] and Chan, Arora, and Ohl [11] consider gas transport only in the immediate vicinity of the nanobubble. When the liquid is supersaturated—necessary for bubble nucleation—line pinned surface nanobubbles can become indefinitely stabilized, a satisfying conclusion consistent with their seemingly infinite lifetimes [12]. However, numerous experimental observations contradict the pinning-oversaturation hypothesis, including that nanobubbles cannot survive in liquid equilibrated to atmospheric pressure, a condition easily achieved in experiments [13]. Nanobubbles even survive incubation for hours in undersaturated liquid [9,14,15]. Moreover, because the model is based on an exact solution for a spherical cap bubble, the resulting dynamics follows the *local diffusive timescale* $\tau_L \sim L^2/D \sim \mu$s (where L is the footprint radius [Fig. 1(a)]). Yet, nanobubbles in experiments respond to changes in gas concentrations over tens of minutes [16] to hours [9,13,14], differing by τ_L by orders of magnitude.

The discrepancy between the two perspectives arises because each implicitly forces a choice of working in either the bubble's or the bulk liquid's operating length and timescales. In this Letter, we combine both perspectives into a unified description that accurately captures both equilibrium and dynamic properties of surface nanobubbles.

We begin with the global gas transport problem considered by Weijs and Lohse [7]. Consider a semi-infinite pool of liquid that rests upon a solid substrate; see Fig. 1(a). As the liquid pool (thickness ℓ) is finite only in one dimension (z), diffusion in this semi-infinite geometry obeys

$$\frac{\partial c}{\partial t} = D\frac{\partial^2 c}{\partial z^2}, \tag{1}$$

where c is the dissolved gas concentration and z is the separation from the substrate. Next, we define the boundary conditions (BC) at the spatial extremities of the computational domain. At the interface between the liquid pool and the external world, the concentration has the fixed value

$$c(z = \ell) = c_i. \tag{2}$$

Under typical conditions, the dissolved gas concentration is at saturation, i.e., $c_i = c_{\mathrm{sat}} = P_0/k_H$ (where k_H is Henry's

constant). In the Weijs-Lohse model, the BC at the solid substrate is directly coupled to the bubble's pressure, but this leads to the incorrect conclusion that the nanobubbles will eventually dissolve [8]. Instead, we prescribe

$$\left.\frac{\partial c}{\partial z}\right|_{z=0} = 0, \tag{3}$$

as the substrate is an impermeable boundary. The problem is closed by defining an initial concentration profile $c(z, t = 0)$.

To model an experiment under laboratory conditions, we assume that at $t = 0$ the liquid is homogeneously oversaturated to $c_0 = 1.5c_{\mathrm{sat}}$ and equilibrates to exact saturation $c_i = c_{\mathrm{sat}}$. From Eqs. (1)–(3), we obtain concentration profiles $c(z, t)$, which we plot at intervals of 60 s in Fig. 1(c). We track $c_0(t) = c(z = 0, t)$ [Fig. 1(d)], whose utility will be apparent later. If $\ell = 1$ mm, the bulk liquid becomes fully equilibrated with the external world over the timescale $\tau_G \sim \ell^2/D \sim 1000$ s or 15 min and reaches ~10 hr if $\ell \sim 1$ cm.

Next, we consider the local gas transport problem in the nanobubble's vicinity, shown in Fig. 1(b). Adapting Popov's theory—originally used to model droplet evaporation [17,18]—for nanobubbles, Lohse and Zhang [10] defined the following boundary conditions. The BC at the bubble interface is given by Laplace's and Henry's laws, i.e., $c_{\mathrm{bub}} = (P_0 + 2\gamma/R)/k_H$, while in the far field the *bulk liquid* concentration holds the fixed value c_0. Defining the oversaturation $\zeta = c_0/c_{\mathrm{sat}} - 1$ and setting $c_{\mathrm{bub}} = c_{\mathrm{sat}}$, one obtains [10]

$$\zeta = 2\gamma \sin\theta_e / LP_0, \tag{4}$$

where θ_e is the equilibrium contact angle and γ is surface tension. Equation (4) has some problematic implications. For example, as it is positive definite, nanobubbles cannot exist under ambient ($\zeta = 0$) or undersaturated ($\zeta < 0$) conditions. Moreover, when compared against experiments, Eq. (4) predicts unrealistically large bulk supersaturations [13,19] of $\zeta > 5$–10; a water-ethanol exchange produces $\zeta \approx 1.85$ *at most* [20].

Recently, we proposed a simple modification [21] to the pinning-oversaturation model that resolves the above-mentioned objections. Nanobubbles typically nucleate on hydrophobic substrates, which preferentially draw gas molecules over liquid. If this attraction can be cast as a potential $\phi(z)$, the distribution of dissolved gas obeys [22]

$$c(z) = c_0 \exp\left(-\frac{\phi(z)}{k_B T}\right). \tag{5}$$

In Fig. 1(e), we plot the localized concentration fields induced by two hydrophobic attraction potentials, as implied by Eq. (5): (a) a short-ranged hydrophobic potential $\phi_h(z) = \phi_0 e^{-z/\lambda}$, where $\phi_0 < 0$ and the interaction distance is $\lambda = 1$ nm, and (b) a van der Waals potential $\phi_v(z) = A/z^9 - B/z^3$, utilizing the parameters A and B for an interaction between a typical gas and hydrophobic solid that has been suggested by Yasui *et al.* [23]. In potential-free regions far from the substrate, $c(z \gg \lambda) = c_0$.

With a spatially varying oversaturation surrounding the bubble, it can be shown that the bubble's dynamical equation is generalized to [21]

$$\frac{d\theta}{dt} = -\frac{Dc_{\mathrm{sat}}}{2\rho_g L^2 h}(1+\cos\theta)^2 f(\theta) \int_0^h \left(\frac{2\gamma}{LP_0}\sin\theta - \zeta(z)\right) dz, \tag{6}$$

where P_0 is atmospheric pressure, ρ_g is the density of the gas, $f(\theta)$ is a geometric factor from Popov's solution [17], and c_{sat} is the saturation concentration of the dissolved gas. The bubble height h can be expressed in θ using $h = L\sqrt{(1-\cos\theta)/(1+\cos\theta)}$.

Equation (6) is solved for a nanobubble for $L = 100$ nm and an initial contact angle $\theta(t = 0) = 5°$ for ϕ_v and ϕ_h for $\phi_0/k_BT = -1$ (hydrophobic) and $\phi_0/k_BT = 0$ (Lohse-Zhang model), and following Refs. [10,21] we assume $D = 2\times10^{-9}\,\mathrm{m^2/s}$, $c_{\mathrm{sat}} = 0.017\,\mathrm{kg/m^3}$, and $\rho_g = 1.165\,\mathrm{kg/m^3}$. The liquid is at saturation $c_0 = c_{\mathrm{sat}}$ in the far field. The dynamics of surface nanobubbles under Eq. (6) are shown in Fig. 1(f), which shows that the nanobubble is unstable at zero potential but stabilized by ϕ_h and ϕ_v. We note, however, that all three analytical curves differ from an exact numerical solution to the diffusion equation, as pointed out recently by Zhu *et al.* [24]. This originates from the fact that both Refs. [10,21] solve the diffusion equation in the quasistatic limit (i.e., the Laplace equation) in order to achieve an analytically tractable form. However, we stress—and it is confirmed in Ref. [24]—that the principal conclusions of both Refs. [10,21] are unaltered, because the equilibrium θ is unaffected by the use of the quasistatic approximation; the dissolution timescale τ_L remains ~μs.

How does the stabilization work? Nanobubbles have the largest surface area at their footprints. The gas-enriched reservoir provides an influx of gas for $z < \lambda$ that can compensate for outfluxes at $z > \lambda$. This effect becomes even more pronounced as the bubble shrinks—a larger proportion of the bubble is within the supersaturated zone, the presence of which leads to stable equilibrium [11]. And what is the evidence that substrate hydrophobicity influences stability and dynamics? Molecular simulations have recently demonstrated that substrate hydrophobicity enhances nanobubbles' resilience to dissolution [25], while nucleation experiments with AFM show that the contact angles of nanobubbles increases with substrate hydrophobicity [26], as we predict [21].

Despite its ability to account for nanobubble properties at equilibrium, our model in Ref. [21] does not correctly capture the dynamic response of nanobubbles, which is in

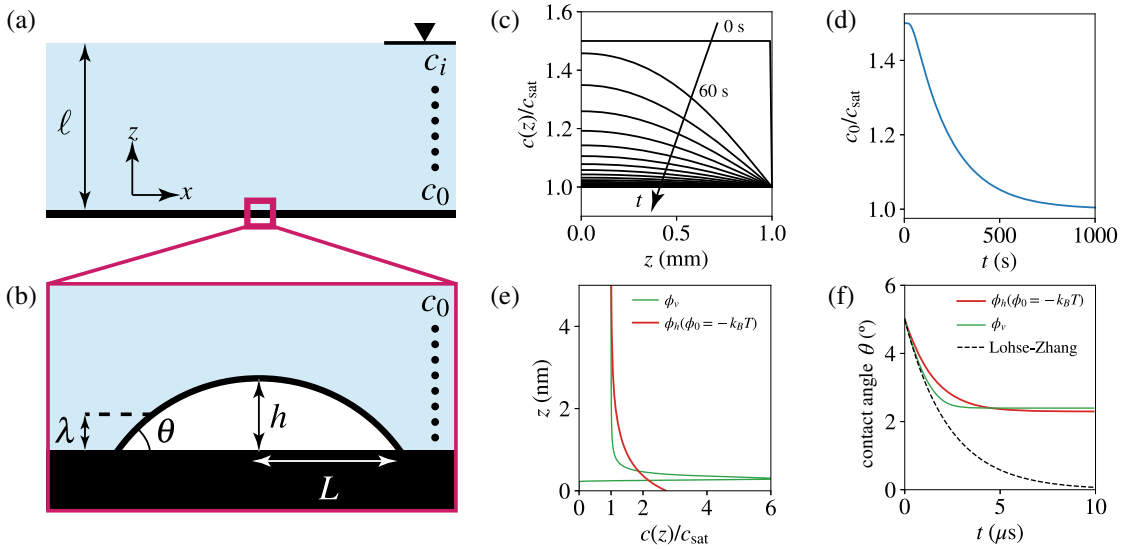

FIG. 1. Two perspectives of nanobubble stability. (a) The global perspective considers transport from bulk liquid to the external world through a semi-infinite pool of thickness ℓ. (b) The local perspective focuses on gas transport surrounding a nanobubble. We assume that the substrate possesses a hydrophobic attraction ϕ with interaction distance λ; note that $c(z \gg \lambda) = c_0$. (c) Numerical solution of the global problem [Eqs. (1)–(3)], for $\ell = 1$ mm and $c_i = c_{sat}$. Concentration profiles $c(z)$ are captured every 60 s, from top to bottom. (d) Temporal evolution of c_0/c_{sat}, the leftmost point of each curve in (c). (e) For common potentials such as van der Waals (green line) or the short-range hydrophobic attraction (red line), $\lambda \sim 1$ nm. (f) The dynamics of a gas nanobubble with $L = 100$ nm under atmospheric conditions ($c_0/c_{sat} = 1$ or $\zeta = 0$) with short-range hydrophobic attraction $\phi_0/k_BT = -1$ (red line), van der Waals (green line), or zero potential (Lohse-Zhang model [10], dashed line). The gas concentration in the far field is exactly saturated $c_0 = c_{sat}$. Note the substantial (8 orders') difference in timescales between (d) and (f).

practice orders of magnitude slower than our model predicts. Our approach is to couple the local and global theoretical perspectives. First, we couple the problems in space by assigning the "bulk concentration" in the local problem c_0 to the substrate concentration in the global problem [Figs. 1(a) and 1(b)]. This coupling assumes that any buildup of gas within $z \leq \lambda \ll \ell$ of the substrate contributes negligibly to global gas transport. Next, the problems are coupled in time. Consider that the local gas concentration around the nanobubble [Figs. 1(a) and 1(b)] at some time is $c_0(t)$. Since $\tau_G \gg \tau_L$, we assume that, when the system has $c_0(t)$, the nanobubble has already reached its equilibrium contact angle θ_e. In other words, there is no need to calculate θ_e by solving the full ordinary differential equation in Eq. (6); rather, we solve for its critical point

$$\int_0^h \left(\frac{2\gamma}{LP_0} \sin\theta - \zeta(z) \right) dz = 0. \tag{7}$$

The long-time dynamics of the nanobubble is evaluated by solving $c_0(t)$ with Eqs. (1)–(3) and using Eq. (7) to obtain $\theta(t)$.

Equilibration.—First, we investigate how a nanobubble would behave in a typical experiment. Surface nanobubbles typically require a supersaturated environment to nucleate [5], so in Fig. 2(a) we consider that c_0/c_{sat} initially has a spatially uniform [e.g., topmost curve in Fig. 1(c)] supersaturated value ($c_0/c_{sat} > 1$) and model equilibration to

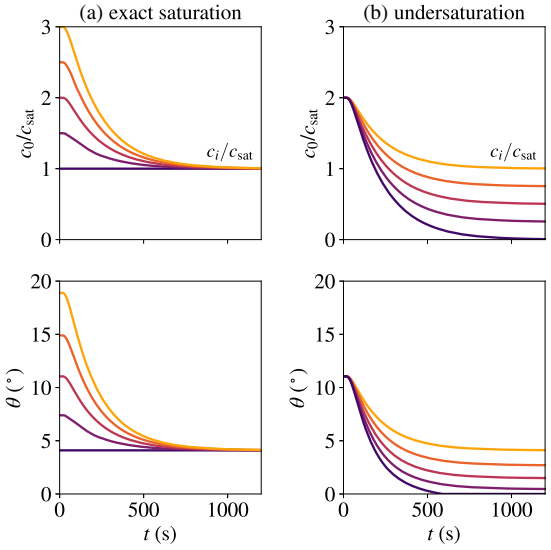

FIG. 2. The long-time dynamics of nanobubbles under equilibration and undersaturation as predicted by the combined model. We assume the short-ranged hydrophobic potential ϕ_h, for $\phi_0/k_BT = -2$, $\lambda = 1$ nm, and $L = 200$ nm. (a) Equilibration to atmospheric conditions is investigated with the liquids initially supersaturated to various degrees $1 < c_0/c_{sat} < 3$. (b) The nanobubbles' response to undersaturation is investigated with the liquids at a common supersaturation of $c_0/c_{sat} = 2$ and compelling the liquid to relax to various degrees of undersaturation $0 < c_i/c_{sat} < 1$. In all cases, except the bottommost curves in (b), the nanobubble attains an equilibrium contact angle after τ_G and remains there indefinitely.

atmospheric conditions by fixing $c_i = c_{\mathrm{sat}}$. The evolution of $c_0(t)$ and $\theta(t)$ for nanobubbles in these conditions is shown in Fig. 2(a). Surface nanobubbles evolve over the global timescale τ_G, reaching an equilibrium when $c_0 = c_{\mathrm{sat}}$. The plots agree with experiments by An *et al.* [13] finding that nanobubbles exhibit substantial changes within several hours of nucleation, before remaining largely invariant for days afterward.

Undersaturation.—Next, we study how nanobubbles dynamically respond in undersaturated conditions. In Fig. 2(b), we plot the substrate-side gas concentration $c_\infty(t)$ and the nanobubble's contact angle $\theta(t)$ evolving as an initially supersaturated liquid relaxes towards different degrees of undersaturation, implemented by modifying the boundary condition at the liquid-gas interface [Eq. (2)] such that $0 < c_i/c_{\mathrm{sat}} < 1$.

The nanobubbles' dynamic response to undersaturation is similar to their response to equilibration—again, they shrink over timescale τ_G to a new and lower contact angle, where they then remain indefinitely. This behavior is consistent with experimental observations of nanobubbles [9] incubated in an undersaturated environment for hours.

Tolerance to undersaturation.—A key feature of the dissolution curves [Fig. 3(b), lower] is that nanobubbles do not simply dissolve once the dissolved gas concentration

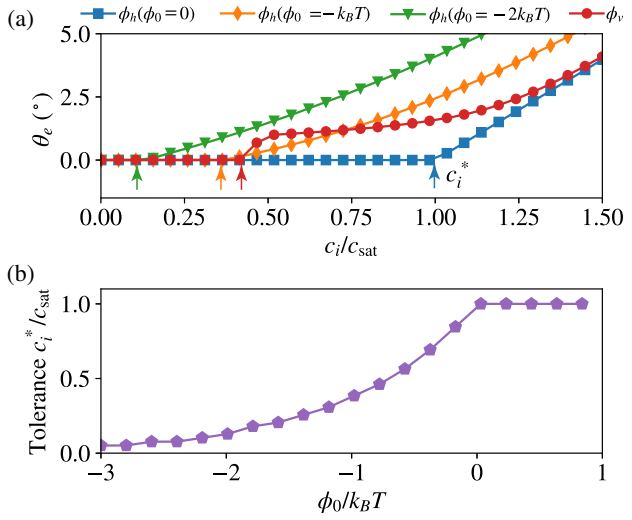

FIG. 3. How surface nanobubbles ($L = 200$ nm) resist undersaturated conditions. (a) The equilibrium angle of a nanobubble as a function of the dissolved gas concentration coupled from the external environment, c_i/c_{sat}, for different interactions: short-range hydrophobic attraction ϕ_h for $\phi_0/k_BT = 0, -1, -2$ and van der Waals ϕ_v. The tolerance to undersaturation, c_i^*, is defined as the largest c_i for which the equilibrium angle $\theta_e = 0°$; c_i^* for each potential is indicated by arrows. (b) Systematically adjusting the strength of ϕ_h resolves the development of tolerance as a function of hydrophobicity ($\phi_0 < 0$ for a hydrophobic substrate). Nanobubbles immediately dissolve under any degree of undersaturation for zero potential (Lohse-Zhang theory) or hydrophilic potentials.

falls below c_{sat}. This is a manifestation of *tolerance*, c_i^*, which we define as the largest c_i for which $\theta_e = 0°$. To determine the tolerance of a hydrophobic substrate, we solve Eq. (7) for various potentials as a function of c_i/c_{sat}, including ϕ_h (strengths $\phi_0/k_BT = 0, -1, -2$) and ϕ_v [Fig. 3(a)], with c_i^*/c_{sat} being the x intersect of each curve. A surface nanobubble with $L = 200$ nm has tolerance $c_i^*/c_{\mathrm{sat}} \approx 0.3$–$0.4$ for ϕ_v and ϕ_h with $\phi_0/k_BT = -1$.

Tolerance to undersaturation is a reproducible experimental feature of surface nanobubbles. On atomically flat graphite, nanobubbles survive a modest undersaturation [9] to $c_i/c_{\mathrm{sat}} \approx 0.9$ yet dissolve under a substantial undersaturation [14] of $c_i/c_{\mathrm{sat}} \approx 0.1$; thus, $c_i^*/c_{\mathrm{sat}} > 0.1$. More recently, Qian, Craig, and Jehannin [15] have found that, for nanobubbles on a silanized silicon wafer, $c_i^*/c_{\mathrm{sat}} < 0.19$. Even though tolerance to undersaturation has been known for over a decade [14], major theories in the literature predict that surface nanobubbles will immediately dissolve under any degree of undersaturation; overall, little effort has been made to understand the mechanistic origin of the tolerance.

In our model, the tolerance to undersaturation arises directly from substrate hydrophobicity, which we show in Fig. 3(b) by varying the strength ϕ_0 of ϕ_h across $-3 < \phi_0/k_BT < 1$. For zero potential (i.e., Lohse-Zhang model [10]) or a hydrophilic substrate, the nanobubble unconditionally dissolves in undersaturated liquid. But as the hydrophobicity increases, $c_i^*/c_{\mathrm{sat}} \to 0$ asymptotically, at which limit gas molecules cannot be destabilized by any degree of degassing. Furthermore, the idea that tolerance develops from substrate hydrophobicity has recently been confirmed in molecular dynamics simulations [25]. Finally, the slow approach to $c_i^*/c_{\mathrm{sat}} \to 0$ in the hydrophobic limit in Fig. 3(b) indicates that the tolerance is below 50% saturation and remains approximately constant over potential strengths $\phi_0/k_BT < -1$. This suggests that a wide variety of hydrophobic substrates should exhibit a strong and approximately uniform tolerance to undersaturation. We anticipate that our predictions can be tested in the near future against, e.g., AFM experiments in which the degree of undersaturation is carefully controlled and increased over many hours (or even days). While the c_i^* of widely used substrates are currently known only to broad ranges, we envisage that systematic studies will be able to narrow c_i^* down to precise, substrate-specific values.

In conclusion, our Letter unifies local and global transport models for surface nanobubbles within a single description that can now simultaneously account for their behavior at equilibrium and as they dynamically approach equilibrium. This model also accounts for a puzzling feature that has long been observed in the literature but not explained—that nanobubbles on hydrophobic substrates exhibit a finite tolerance to undersaturation.

Given the florid terms ("minute miracles" [27]) with which surface nanobubbles have been described, it might

be expected that a viable explanation for their stability and dynamics may require novel or unexpected physics. To the contrary, the strong agreement our model achieves with the experiment hinges on a careful quantification of gas transport at the local and global scales and requires only reasonable and well-accepted assumptions such as contact line pinning, well-defined diffusion length scales, and substrate hydrophobicity.

We thank Detlef Lohse and Drew F. Parsons for discussions and advice. B. H. T. acknowledges support from the SMART Fellowship, and H. A. from the ARC Future Fellowship.

*hjan@ntu.edu.sg
†claus-dieter.ohl@ovgu.de

[1] J. R. T. Seddon, D. Lohse, W. A. Ducker, and V. S. J. Craig, Chem. Phys. Chem. **13**, 2179 (2012).
[2] V. S. J. Craig, Soft Matter **7**, 40 (2011).
[3] J. R. T. Seddon and D. Lohse, J. Phys. Condens. Matter **23**, 133001 (2011).
[4] M. Alheshibri, J. Qian, M. Jehannin, and V. S. J. Craig, Langmuir **32**, 11086 (2016).
[5] D. Lohse and X. Zhang, Rev. Mod. Phys. **87**, 981 (2015).
[6] P. S. Epstein and M. S. Plesset, J. Chem. Phys. **18**, 1505 (1950).
[7] J. H. Weijs and D. Lohse, Phys. Rev. Lett. **110**, 054501 (2013).
[8] P. Ball, Chem. World (2013).
[9] X. Zhang, D. Y. C. Chan, D. Wang, and N. Maeda, Langmuir **29**, 1017 (2013).
[10] D. Lohse and X. Zhang, Phys. Rev. E **91**, 031003(R) (2015).
[11] C. U. Chan, M. Arora, and C.-D. Ohl, Langmuir **31**, 7041 (2015).
[12] It is popularly stated in the literature that surface nanobubbles survive for at least several weeks [1–3,5]. This statement *does not* imply that surface nanobubbles have a finite lifetime. It merely means that they comfortably survive—showing no imminent sign of dissolution—for as long as researchers have bothered to wait.
[13] H. An, B. H. Tan, Q. Zeng, and C.-D. Ohl, Langmuir **32**, 11212 (2016).
[14] X. H. Zhang, G. Li, N. Maeda, and J. Hu, Langmuir **22**, 9238 (2006).
[15] J. Qian, V. S. J. Craig, and M. Jehannin, Langmuir **35**, 718 (2019).
[16] S. R. German, X. Wu, H. An, V. S. J. Craig, T. L. Mega, and X. Zhang, ACS Nano **8**, 6193 (2014).
[17] Y. O. Popov, Phys. Rev. E **71**, 036313 (2005).
[18] H. Gelderblom, A. G. Marín, H. Nair, A. van Houselt, L. Lefferts, J. H. Snoeijer, and D. Lohse, Phys. Rev. E **83**, 026306 (2011).
[19] X. Li, Y. Wang, B. Zeng, Y. Li, H. Tan, H. J. Zandvliet, X. Zhang, and D. Lohse, Langmuir **34**, 10659 (2018).
[20] H. An, G. Liu, R. Atkin, and V. S. J. Craig, ACS Nano **9**, 7596 (2015).
[21] B. H. Tan, H. An, and C.-D. Ohl, Phys. Rev. Lett. **120**, 164502 (2018).
[22] M. P. Brenner and D. Lohse, Phys. Rev. Lett. **101**, 214505 (2008).
[23] K. Yasui, T. Tuziuti, W. Kanematsu, and K. Kato, Phys. Rev. E **91**, 033008 (2015).
[24] X. Zhu, R. Verzicco, X. Zhang, and D. Lohse, Soft Matter **14**, 2006 (2018).
[25] Y.-X. Chen, Y.-L. Chen, and T.-H. Yen, Langmuir **34**, 15360 (2018).
[26] Z.-L. Zou, N.-N. Quan, X.-Y. Wang, S. Wang, L.-M. Zhou, J. Hu, L.-J. Zhang, and Y.-M. Dong, Chin. Phys. B **27**, 086803 (2018).
[27] P. Ball, Chem. World **9**, 60 (2012).